EUROGRAPHICS - IEEE VGTC Symposium on Visualization (2005)
K. W. Brodlie, D. J. Duke, K. I. Joy (Editors)

Interactive Visualization for Neck-Dissection Planning

Arno Krüger[1] Christian Tietjen[1] Jana Hintze[1] Bernhard Preim[1] Ilka Hertel[2] Gero Strauß[2]

[1] Department of Simulation and Graphics
Otto-von-Guericke-University of Magdeburg, Germany
{krueger|tietjen|hintze|preim}@isg.cs.uni-magdeburg.de

[2] ENT Department
University Hospital of Leipzig, Germany
Ilka.Hertel|strg@medizin.uni-leipzig.de

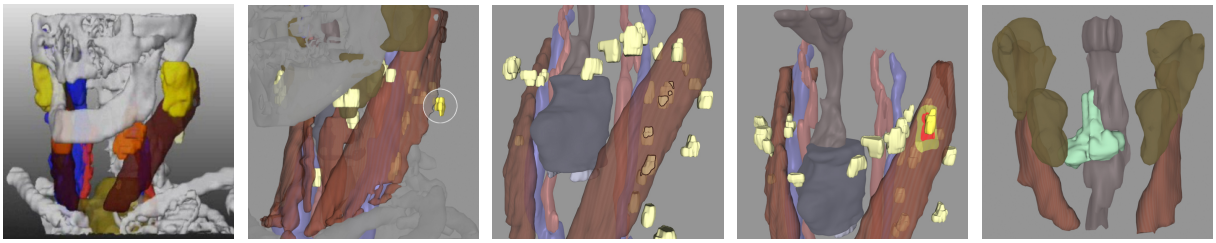

Abstract

In this paper, we present visualization techniques for neck dissection planning. These interventions are carried out to remove lymph node metastasis in the neck region. 3d visualization is intended to explore and to quantify anatomic and pathologic structures and thus support decisions concerning the surgical strategy. For this purpose we developed and combined visualization and interaction techniques such as cutaway views, silhouettes and color-coded distances. In addition, a standardized procedure for processing and visualization of the patient data is presented.

Categories and Subject Descriptors (according to ACM CCS): I.3.6 [Computing Methodologies]: Computer GraphicsMethodology and Techniques; I.4.m [Computing Methodologies]: Image Processing and Computer VisionMiscellaneous; J.3 [Computer Applications]: Live and Medical SciencesHealth;

Keywords: Medical visualization, neck dissection, operation planning, lymph node exploration

1. Introduction

Neck dissections are carried out for patients with malignant tumors in the head and neck region. These surgical procedures are necessary because the majority of the patients develops lymph node metastases in the neck region.

The extent of the intervention depends on the occurrence and location of enlarged (and probably) malignant lymph nodes. In particular, the infiltration of a large muscle (*M. sternocleidomastoideus*), a nerve (*N. facialis*) or blood vessel determine the surgical strategy. If for example the *A. carotis interna* is infiltrated, the patient is regarded as not resectable. The identification and the quantitative analysis of lymph nodes with respect to size and shape is crucial for the surgeon's decision. The image analysis and visualization techniques described in this paper support decisions regarding the resectability and the surgical strategy for neck dissections.

Visualization techniques aim at comprehensible renderings of the relevant information. This includes the visualization of the target structures and some context information necessary to illustrate the spatial relations. By means of our visualizations, we convey information concerning shape and size of lymph nodes, as well as critical distances or even infiltrations of lymph nodes into important structures. In addition to carefully parameterizing surface rendering, we explore silhouette rendering and cutaway views for parts of an object's surface. Although these visualizations are targeted at neck dissection planning they are applicable to other applications such as the evaluation of lung nodules. We also discuss interaction facilities to explore the data. In particular, we discuss the selection of lymph nodes based on their properties. Our case study report is based on 18 clinical CT-datasets which have been acquired and processed for the planning of neck dissections.

2. Image Analysis

In order to support neck dissection planning, it is crucial to segment the relevant anatomic and pathologic structures. The segmentation is a prerequisite for the selective visualization and the quantitative analysis of the patient data. For surgical planning, the extent of pathologic structures, distances to important anatomic structures and the potential infiltration are of special interest.

2.1. CT Data

We employed 18 CT-datasets which have been acquired for neck dissection planning. Eleven of these datasets contained a tumor in the head and neck region and were suspected of containing lymph node metastases as well. The quality of the datasets was diverse with respect to the signal-to-noise ratio, motion artifacts as well as the slice distance (0.7 to 3 mm), resulting from different CT scanning devices and acquisition parameter.

The data were exchanged based on a WWW upload including information concerning the diagnosis of the patient and specific requirements for computer-supported planning.We choose not to employ MRI data, although they are wide-spread for diagnosis in the neck region due to their inherent inhomogeneity and low resolution.

2.2. Requirements

In collaboration with our clinical partners, the target structures of the segmentation were identified as being most relevant for preoperative planning:

- Vascular structures (*V. jugularis, A. carotis*)
- Muscles (*M. sternocleidomastoideus*)
- Skeletal structures (*Mandible* and *Clavicle*)
- Salivary glands (*Gl. submandibularis, Gl. parotidea*)
- *Pharynx*
- *N. accessorius* (where visible),
- Primary tumor,
- Lymph nodes, with emphasis on enlarged and potentially malignant nodes.

In selected cases, the segmentation of additional structures is desirable, e.g. additional muscles or nerves.

2.3. Segmentation

Segmentation was carried out by means of the software platform MeVisLab (MeVis, Bremen, http://www.mevislab.de), a library which provides a variety of image preprocessing and segmentation methods. A live wire approach was employed for the segmentation of muscles (*M. sternocleidomastoideus, M. omohyoideus*) and the salivary glands. With this semi-automatic approach, the user selects seedpoints and the system calculates a path of minimal cost in between. This procedure is carried out in selected slices; the intermediate contours are interpolated [SPP00]. The interactive watershed transform [HP03] proved to be suitable to identify and delineate the *V. jugularis* and *A. carotis*. Intensity-based region growing was used for bone and *Pharynx* segmentation.

While the muscles and the glands could be identified in the majority of the datasets, most of the desired nerves could not be identified due to their size in relation to the image resolution. Among the vascular structures, only the *A. carotis* and *V. jugularis* could be segmented in most of the data.

Nerves are very difficult to detect in CT-images because they are very small. In datasets with a large slice distance (>3 mm), they could not be detected at all. In CT-data with low slice distance, the *N. accessorius* and *N. vagus* could be identified manually in a few slices. Due to the low slice distance the partial volume effect (averaging of signal intensities in a volume element) is less disturbing. As the approximate course of these nerves is essential for surgeons, we chose to segment the nerves partially and to employ this information for an approximate visualization (see Section 6).

Primary tumors were segmented manually as well. They exhibited low contrasts and could only be distinguished by exploiting considerable anatomic knowledge, in particular symmetry considerations. At present, also the lymph nodes are identified manually. Our ongoing research aims at an automatic detection of lymph nodes, using assumptions regarding their grey values, size and shape. The segmentation is described in more detail in [HCP*05].

3. Visualization of the Segmented Target Structures

We discarded volume rendering because it does not provide essential information for our purposes. By relying on surface visualizations, we provide all necessary information within rather small surface models which can be easily transmitted over the internet and explored using wide-spread software. In addition we use functionalities from modern graphics hardware (GPU) which is optimized for surface rendering.

3.1. Color Selection

Our color selection was guided by observations from textbooks [Net02] and later refined in discussions with the clinical partners. Transparency was primarily used to expose important structures, such as lymph nodes. This type of visualization is shown in Figure 1.

After processing three CT-datasets, we evaluated all visualization parameters. In several in-depth discussions, we modified colors and transparencies for all structures to enhance contrasts and recognizability of object borders. As a result, a final color table was developed which represents our standardization (see Table 1). Finally, all datasets have been adapted to these values.

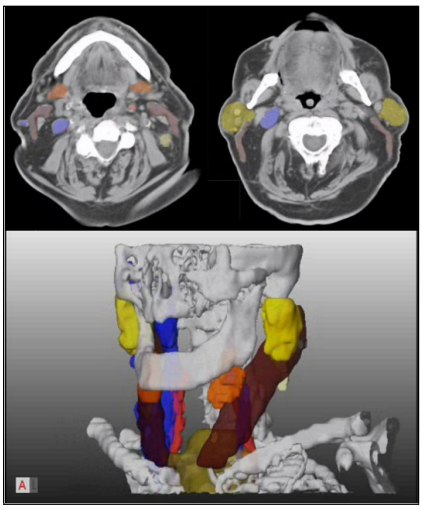

Figure 1: *2d and 3d visualizations are combined for neck dissection planning. The colors used in the 3d visualization are also used to superimpose segmentation results in 2d slice data.*

3.2. Material Effects for the Visualization

It turned out that object-based transparency specification does not allow a comprehensible visualization of complex structures. With multiple highly transparent objects, the specific location of a target object is barely visible with a high opacity on the other hand the spatial relations between emphasized objects are difficult to recognize (see Fig. 2).

The key for the solution is employing object-based opacity maps with alternating opaque and semi-transparent stripes. They are mapped to the neck muscles in roughly the same direction as real fibers. For this purpose we use the calculated envelope of each muscle and compute its bounding cylinder. By using the normals of the muscle we transfer the texture coordinates from the cylinder to each vertex of the muscle. With this technique the real texturing of neck muscles is slightly indicated in the visualization. In [DCLK03] the identification of muscle fibres for hatching is presented. This technique was found to be too complex for our purposes, since neck muscles are regarded as context information only.

Structure	Red	Green	Blue
A. carotis	240	50	50
V. jugularis	80	80	250
Muscles	100	40	20
Skeletal structures	255	255	255
Salivary glands	180	150	110
Pharynx	255	190	150
Nerves	240	185	80
Primary tumor	255	255	200
Lymph nodes	255	255	150

Table 1: *Color table for the standardized visualization of neck structures*

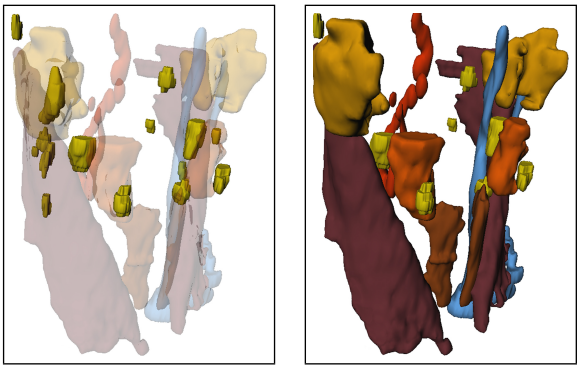

(a) Neck structures drawn too transparent. (b) Neck structures opaque.

Figure 2: *With object-based transparency assignment, the location of lymph nodes cannot be depicted effectively.*

To improve the visibility of lymph nodes and tumors, all colors from other objects are reduced in saturation and lightness. Especially skeletal structures are invisible during surgery and provide only spatial orientation, e.g. *Mandible* and *Clavicle* serve as landmarks. In Figure 3, the improved color selection for lymph node emphasis is shown.

Inspired by illustrations from textbooks [Net02], we use a material with shiny impression for vascular structures. This technique enhances the recognizability of vascular structures (cf. Fig. 3 or 6).

Segmented objects from clinical datasets mostly exhibit unnatural artifacts. Therefore we smoothed all objects visually (not geometrically), by assigning a slight self-illumination (emissive color in an SoMaterial node of OpenInventor) to these objects. This effected a visual flatness of the surface because the shading does not render hard contrasts (see the bones in Fig. 3 and 5).

Further visualization techniques were investigated. The use of silhouettes for highly transparent objects considerably increases the recognizability. As a result, silhouettes are used e.g. to enhance strongly transparent objects (see Fig. 3). We do not consider hatching as a promising technique for surgery planning. It seems to be challenging to reliably derive appropriate hatching parameters from the complex geometries of segmented objects. The improved spatial understanding is probably not significant to justify additional interaction effort.

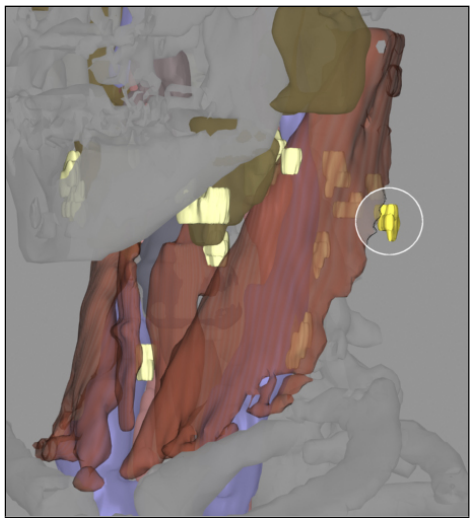

Figure 3: *Emphasized lymph node partially behind the M. sternocleidomastoideus. Note the use of a cutaway view as well as the thin silhouette line to enhance depth perception.*

In contrast, the use of cutaway views is promising. As an example, a muscle which is covering a tumor should be rendered only transparent in regions, where the tumor is behind. In Section 4.2 the use of cutaway views is presented.

3.3. Integrating Measurement in Neck Dissection Planning

Measurement tools to compute the extent of anatomic structures and the distance between structures are also provided [PTSP02]. With these tools (see Fig. 4), the extent of enlarged lymph nodes can be determined precisely. The measurements are directly included in the 3d visualization.

4. Interaction Techniques for Exploring Lymph Nodes

The exploration of a complex set of enlarged and therefore surgically relevant lymph nodes requires appropriate interaction techniques. The usual selection of objects via their name is not feasible. The selection of entire lymph node groups or via measurement results is more appropriate. Extent or minimal distances to risk structures are possible criteria. Two problems related to lymph nodes are essential for surgery planning: the exploration of enlarged lymph nodes (partly over 20) and the evaluation of infiltration or resectability of lymph nodes.

4.1. Sequential Visualization of Lymph Nodes

The basic interaction for the exploration of lymph nodes is the selection. We suggest a facility to step through all lymph nodes with a simple interaction. We found that the most interesting information are the quantity of enlarged lymph nodes and their potential malignity. Therefore, a simple list, ordered by the lymph node number, is not appropriate for exploration. In our planning tool we provide three different selection criteria - extent, volume or malignity from TNM-classification, discussed in Section 4.5.

As a feedback after selection, lymph nodes should become visible. It is not appropriate to render a large object, such as the *M. sternocleidomastoideus*, highly transparent, to expose a small lymph node. A better alternative is to render only a small part of the muscle transparent which can be achieved by cutaway views (see [VKG04]).

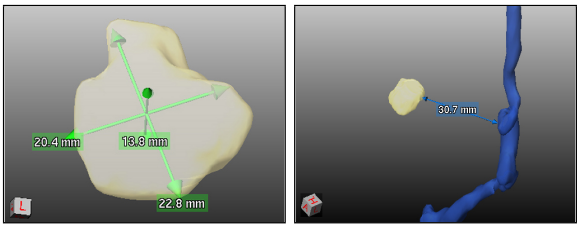

(a) Extension measurement of a tumor, automatically computed via principal axis transformation.

(b) Minimal distance between an enlarged lymph node and the *V. jugularis*.

Figure 4: *Measurement tools for automated computing the extent of structures and minimal distances.*

4.2. Emphasis with Cutaway Views

For the exploration of lymph nodes, we generate a cutaway view with a cylindrical cutting volumen. We calculate the convex hull from the lymph node in 3d and project it via OpenGL to the screen. From the result wie calculate the convex hull in 2d and finally the minimal enclosing circle plus a fixed margin around a lymph node. So with each step we reduce the involved points to enhance the speed. The resulting volume is cutting all structures in front of the lymph node. The cylinder is aligned orthogonal to the viewing plane and is terminated at the lymph node. OpenInventor, OpenGL 2.0 and the fragment shader functionality from modern GPUs is used to realize the cutting of the structures in realtime.

The intersecting parts of foreground objects within the bounding volume are displayed strongly transparent. However, the depth perception is limited in this region. Therefore a thin silhouette (see [IFH*03]) of the muscle is included brightly, calculated simply from the scalar product between viewing vector and the surface normals.

With these visualization parameters, foreground and background objects are correctly perceived. The emphasized area is additionally marked with a bright circle. The radius of this area is the same as the radius of the cutting cylinder. In technical illustrations in contrast, organic shapes or zigzag

should be used to compute cutaway views (see [DWE03]). The lymph node is also visually enhanced by raising the saturation of color (see Figure 3 for the interactive visualization result).

As shown in Figure 5, this combination of visualization techniques is applicable also for multiple occlusions 5(a) or full visibility 5(b). Hence, the surgeon may interactively step through all lymph nodes, e.g. by pressing the tab key. The currently selected object (CSO) will always be clearly emphasized. We chose not to rotate the camera automatically to emphasize the CSO because of distracting effects.

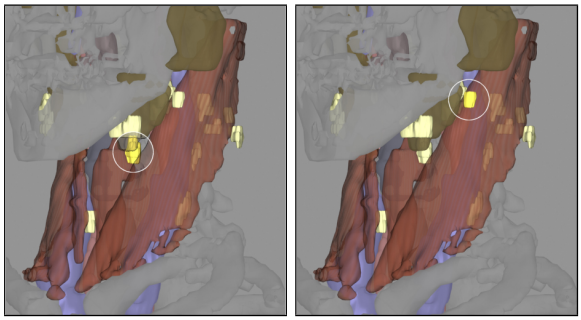

(a) Lymph node behind the *M. sternocleidomastoideus* and the *Gl. submandibularis.*

(b) Lymph node in front of all other structures.

Figure 5: *Combining color, transparency mapping and a cutaway view to emphasize a single lymph node. In the interactive tool the stepping through all lymph nodes is facilitated.*

4.3. Visualizing Distances to Risk-Structures

For the evaluation of the resectability, distances to risk structures are crucial. We employ a distance-dependent coloring of the neck vessels and muscles which conveys the distance to the lymph nodes. With a discrete color scale (gradation: 2 and 5 mm) the resectability of this target may be evaluated.

The emphasized lymph node in Figure 6 is located in front of the *M. sternocleidomastoideus*, where the distance information is displayed. Two depending levels are encoded for the distance. For a well-defined separation of the structures in the 3d scene, the used colors were evaluated by the clinical partners and regarded as appropriate. This kind of accentuation leads to a more simple application for several objects, so the visual focus is located at the CSO. Distance information relating to multiple objects would more likely confuse the viewer.

A color-coding of the distances does not indicate an infiltration of a muscle or a vessel. We employ a line character accentuation (see [TIP05]) of the cut line which is marked above the illustration. In Figure 7, the potential infiltration of the *M. sternocleidomastoideus* is shown. According to

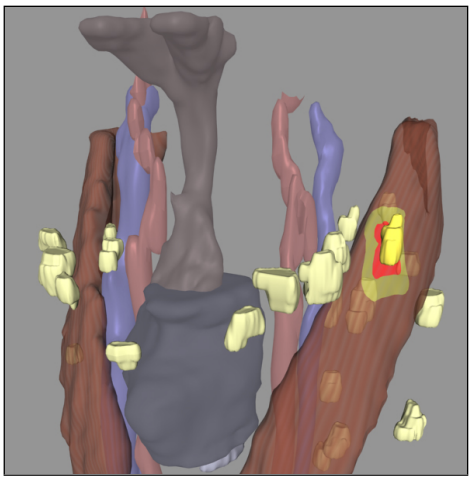

Figure 6: *Color-coded distance of a lymph node to the M. sternocleidomastoideus. The 2 mm distance is coded in red, 5 mm in yellow.*

the segmentation results, these lymph nodes reach into the muscle. In reality it is possible, that the muscle tissue is displaced, but not infiltrated. A displacement occurs considerably more often. Distance-related visualizations may be generated for each anatomic structure. Other relevant examples are the *A. carotis* and the *V. jugularis*.

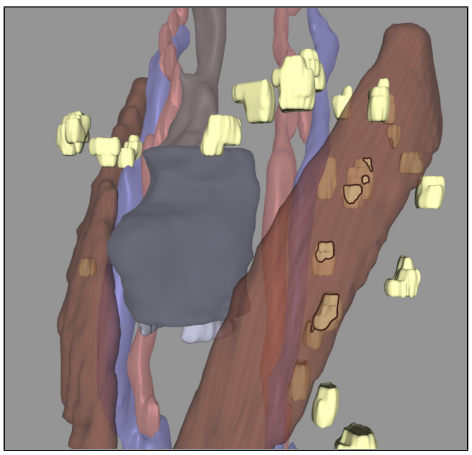

Figure 7: *Possible infiltration of the M. sternocleidomastoideus. Silhouette lines form an intersection line between muscle and lymph nodes.*

A drawback of this visualization technique is, that lymph nodes which are in front and potentially infiltrate the muscle, will not be accentuated in the current viewing position. Therefore the user should rotate the 3d scene. A color-coded view for potentially infiltrating lymph nodes is also provided for a fast overview.

4.4. Visualization of Lymph Node Size

Primarily, the size of lymph nodes is important. Medical doctors consider lymph nodes with an extent of more than 1 cm as critical (potentially malignant) and would resect them. Therefore, we generate an initial visualization which conveys the size of lymph nodes. In Figure 8, this is realized by a front view and color-coded lymph nodes. The color graduation appears via two discrete values: yellow for lymph nodes smaller than 1 cm and turquoise for extents beyond. Here, we emphasize lymph nodes larger than 1 cm minus the slice thickness, to account for possible inaccuracies from image acquisition and segmentation. The maximum extent is used to realize the color-coding. If this value exceeds the calculated threshold, the lymph node will be classified as bigger than 1 cm and is coded as enlarged. A discrete color-coding with more than two grades turns out to be inappropriate, because the surgical decision is of binary nature, too. In the real surgical procedure, all lymph nodes will be removed, that are palpably enlarged.

This visualization is based on data known from the segmentation process. All lymph nodes and tumors are measured automatically by a principal component analysis from which the extent is derived [PTSP02]. We do not calculate the volumes of lymph nodes since high measurement inaccuracies due to very small volumes are to be expected (volumetry is uncertain when a large portion of border voxels occurs).

By a mouse-over interaction, tooltips, respectively text boxes, fade in with the precise measurement values of extent and minimal distances to risk structures (see Fig. 8). For primary tumors the same interaction is provided.

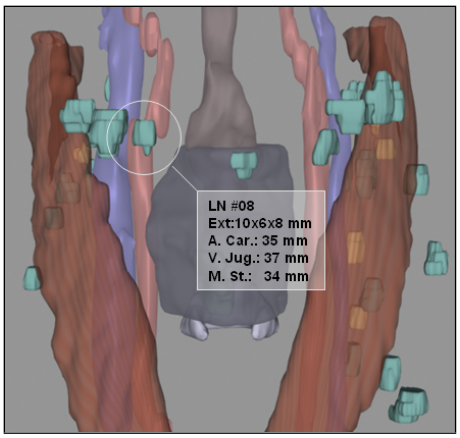

Figure 8: *Color-coded lymph node size. Two levels are used: yellow below 1cm and turquoise above. The exact values are readable via tooltip.*

4.5. Malignity and TNM Classification

Surgeons grade the level of a tumor disease according to a fixed scheme, the TNM classification. It is constructed based on three numerical values, with possible levels for each. T stands for the tumor grade (five levels), N for the lymph node state (N0 or N1) and M for the level of distant metastases (M0 or M1). About the last one we cannot state anything with computer assistance, but the T and N values can be determined algorithmically.

The lower levels of the T-classification (1, 2 and 3) characterize mostly the size of pathological structures. Level 4 and 5 are assigned with respect to the infiltration of critical structures, such as vasculature. An adhesion with a neck arteria tends to a level 5 classification, because such cases are not resectable.

For tumor classification, the computer cannot perform an automatic estimation. The shapes vary strongly and the spatial relationships are too complex. A computer assistance for the surgeon is reasonable: According to the measurement results, the extent can be employed for a suggestion of the T-level is presented. By observing the 3d-visualization and the overlayed segmentation in the CT-slices (see Fig. 1), the surgeon can correct the initial level.

The N part of the classification can be automated. This is reasonable, because of the large number of lymph nodes in most cases. The extent of a lymph node is considered in determining conclusion about malignancy. Spherical structures are more likely malignant than longish ones and their roundness can be calculated by comparing the 3 principal directions.

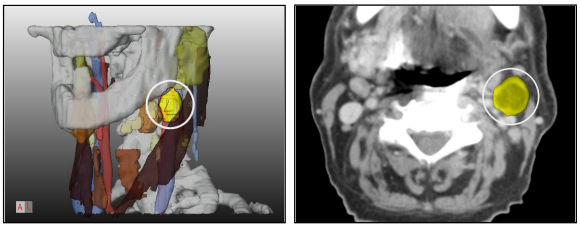

(a) 3d-visualization. (b) Axial CT-slice.

Figure 9: *Representation of a lymph node with a central necrosis marked in 3d and in a 2d view.*

Another clue concerning malignancy is the inner gray value characteristic. A central necrosis has much darker values in the center than on the border. In Figure 9, such a case is shown. Detectable characteristics in gray values can be used for an automated N classification. If required, the suggested TNM is displayed on the screen border in our operation planning tool, like other patient data.

5. The Segmentation and Visualization Process

It was a major goal to produce comparable visualizations for different patient data. Besides the visualization, a procedure

for the treatment of datasets is to be defined. This includes the type and resolution of the datasets, the application of segmentation methods, the type of visualization and the presentation of the results. We consider the following aspects of standardization:

- type and resolution of the processed datasets (CT, < 3 mm slice distance)
- standardized "order sheet" with specifications regarding structures, that should be segmented besides the standard in this case
- technique of segmentation for the different structures
- naming of the structures
- colors, views and types of visualization
- measurement of segmented lymph nodes, tumors and the distances to risk structures
- data exchange and result presentation on the project's web page

The segmentation and visualization is carried out as a service for the surgical partner in the framework of a research project. Patient datasets are always submitted with an "order sheet". By this, the diagnosis is stated and target structures and measurements besides the standard are listed (see Section 2).

The segmentation process is also standardized (sequence of segmentation tasks). However, parameters have to be adapted to each dataset. The result is presented as images and small animation sequences. 2d-slice views with the segmentation results (which are radiologically evaluated) transparently overlaid to the original data were created to support the verification of segmentation results and the mental integration of 3d visualizations with the underlying slice data. Selective clipping of bony structures was used to enhance the interpretation of the spatial relations. The clips, images and interactive 3d-data are available for the project partner via a secured web page.

The average time for image analysis and creation of the visualizations was approximately 90 minutes. Most of the time was spent on the segmentation of lymph nodes.

6. Influence on Surgical Strategies

The visualization results were compared with the experiences of real surgical interventions. The surgeons attested a high degree of correspondence to intraoperative views. In some cases, the results of computer assisted planning were essential for the surgical decision.

For the surgeon it is necessary to evaluate distances to risk structures (see Section 4.4). The number of lymph nodes is employed to develop an understanding of the expected difficulty of the resection. These nodes are not visible in the neck area, but hidden in e.g. fatty tissue.

The above-mentioned information improves neck dissections with respect to speed and safety. In contrast, other information a priori can lead to choose another surgical strategy. If it turns out, that possibly important structures are infiltrated, the involved areas are not resectable, without previous radiation therapy. Therefore, it is important to estimate the resectability as reliably as possible and to choose the right surgical strategy preoperatively. In neck dissections, there are the following strategies: left or right sided and with different kinds of radicality e.g. with resection of muscles.

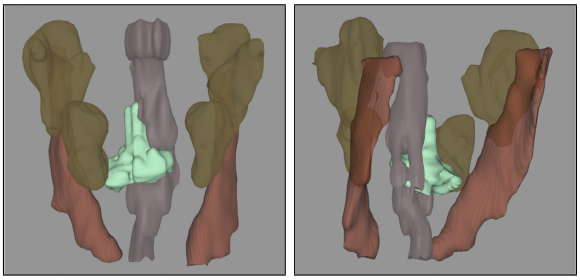

(a) Front view. (b) Back view.

Figure 10: *A large tumor (green) is infiltrating the Pharynx. The upper tail also infiltrates the cranial base.*

Figure 10 presents a case, where the tumor had a long tail, that was not noticeable on CT-slices. Due to the infiltration of the cranial base, the intervention had to be terminated unsuccessfully. The surgeon stated, that having seen the segmentation results in advance might have led to another surgical strategy. Currently, CT-data is acquired close before surgery. There is almost no time for preparing the operation planning.

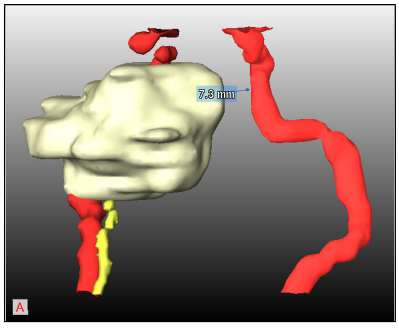

Figure 11: *N. hypoglossus (yellow) and A. jugularis (red). Notice the slice artifacts in the course of the nerve near the tumor (dark yellow).*

Information about the nerves are valuable, because they are often injured and patients carry away heavy intricacies for lifetime. Slice distance concerned in the project is 2-3 mm in average. A higher resolution is required to segment big facial nerves. Even then, only a partial segmentation is feasible, because their size and contrast is too small. This is the case even at the high resolution of the Visible Human

dataset. Similar to [HPP*00], we model the course between selected points of the nerve. Instead of visually appealing B-Splines, we use simple lines with an appropriate thickness. Figure 11 shows such a segmentation result from a 1 mm slice distance data set. The visualization of the approximate course of the nerve was regarded as useful.

7. Conclusion & Future Work

We presented image analysis and visualization techniques for planning neck dissections. The focus of our work is the visualization of enlarged lymph nodes and the surrounding structures. The image analysis which requires considerable experience, is carried out as a service in the framework of a research project. As a result, surgeons are provided with standardized static visualizations and with standardized animation sequences, primarily rotations of different subsets of the relevant target structures. To explore the data themselves, they are provided with an interactive system with surface rendering and measurement facilities.

We attempted a standardized report consisting of images from standardized viewing directions. The correlation between 3d visualizations and the original 2d slices of the radiological data is crucial to assess whether the 3d visualizations are reliable. Therefore segmentation results are indicated as semitransparent overlays to the original CT-data. The potential of 3d visualizations for surgery planning cannot be fully exploited by means of standardization. Each and every case exhibits some peculiarities which require interaction techniques to explore them. In particular, the occurrence, number and size of enlarged lymph nodes differ from patient to patient. Therefore, we developed an "order sheet".

Our work is directed at a progress in planning neck dissections; more reliable preoperative decisions and more safety during the intervention are the primary goals. Our strategies to adjust 3d visualizations, to explore spatial relations, is applicable to other areas of computer assisted surgery. The use of silhouettes as well as the use of cutaway views to expose hidden pathologic structures turned out to be useful for surgery planning. Cutaway views are also useful for the exploration of round lesions (lung nodule) or small liver metastases.

Future work includes an in-depth user study to characterize the impact of 3d visualization on the surgical strategy. In this study, we will compare surgery planning based on conventional information (axial slices of CT-data) with surgery planning based on the additional information which is available after image processing. A specialized further development of the interactive planning tool, the "InterventionPlanner ENT" (ear nose throat), currently will be finished.

Acknowledgments

This work was carried out in the framework of a project supported by the Deutsche Forschungsgemeinschaft (DFG) (Priority Programme 1124, PR 660/3-1). Special thanks go to Jeanette Cordes and Ragnar Bade for good ideas and substantial support on visualization issues. Dr. Uta Preim validated image analysis results as radiologist.

References

[DCLK03] DONG F., CLAPWORTHY G. J., LIN H., KROKOS M. A.: Non-photo-realistic rendering of medical volume data. *IEEE Computer Graphics and Applications 23* (2003), 44–52. 3

[DWE03] DIEPSTRATEN J., WEISKOPF D., ERTL T.: Interactive Cutaway Illustrations. *Computer Graphics Forum 22*, 3 (2003), 523–532. 5

[HCP*05] HINTZE J., CORDES J., PREIM B., STRAUSS G., HERTEL I., PREIM U.: Bildanalyse für die präoperative Planung von Neck dissections. In *Bildverarbeitung für die Medizin 2005* (2005), Informatik aktuell, Springer. 2

[HP03] HAHN H., PEITGEN H.: IWT-Interactive Watershed Transform: A hierarchical method for efficient interactive and automated segmentation of multidimensional grayscale images. In *Medical Imaging 2003: Image Processing* (2003), vol. 5032, SPIE, pp. 643–653. 2

[HPP*00] HÖHNE K. H., PFLESSER B., POMMERT A., RIEMER M., SCHUBERT R., SCHIEMANN T., TIEDE U., SCHUMACHER U.: A realistic model of the inner organs from the visible human data. In *MICCAI* (2000), pp. 776–785. 8

[IFH*03] ISENBERG T., FREUDENBERG B., HALPER N., SCHLECHTWEG S., STROTHOTTE T.: A Developer's Guide to Silhouette Algorithms for Polygonal Models. *IEEE Computer Graphics and Applications 23*, 4 (2003), 28–37. 4

[Net02] NETTER F. H.: *Atlas of Human Anatomy*, 3 ed. ICON Learning Systems, 2002. 2, 3

[PTSP02] PREIM B., TIETJEN C., SPINDLER W., PEITGEN H.-O.: Integration of Measurement Tools in Medical Visualizations. In *Proc. of IEEE Visualization* (2002), pp. 21–28. 4, 6

[SPP00] SCHENK A., PRAUSE G., PEITGEN H.: Efficient Semiautomatic Segmentation of 3D Objects in Medical Images. In *Medical Image Computing and Computer-assisted Intervention* (2000), vol. 1935 of *LNCS*, Springer, pp. 186–195. 2

[TIP05] TIETJEN C., ISENBERG T., PREIM B.: Combining Silhouettes, Surface, and Volume Rendering for Surgery Education and Planning. In *IEEE/Eurographics Symposium on Visualization* (2005), Springer. 5

[VKG04] VIOLA I., KANITSAR A., GRÖLLER M. E.: Importance-driven volume rendering. In *Proc. of IEEE Visualization* (2004), pp. 139–145. 4